Dimethyltin(IV)-4,6-dimethyl-2-pyridylselenolate: An Efficient Single Source Precursor for the Preparation of SnSe Nanosheets as Anode Material for Lithium Ion Batteries

Gourab Karmakar,[a,b] Kruti K. Halankar,[a] Adish Tyagi,*[a,b] B. P. Mandal,[a,b] A. P. Wadawale,[a] G. Kedarnath,*[a,b] A. P. Srivastava[c] and Vishal Singh[c]

[a]*Chemistry Division, Bhabha Atomic Research Centre, Mumbai- 400 085 (India),*

[b]*Homi Bhabha National Institute, Anushaktinagar, Mumbai- 400 094 (India)*

[c]*Materials Science Division, Bhabha Atomic Research Centre, Mumbai- 400 085 (India).*

Email: tyagia@barc.gov.in, kedar@barc.gov.in

Figure captions

Figure S1 . $^{77}Se\{^1H\}$ NMR spectra of bis(4,6-dimethyl-2-pyridyl)diselenide

Figure S2. $^{77}Se\{^1H\}$ NMR spectra of $[Me_2Sn\{2\text{-}SeC_5H_2(Me\text{-}4,6)_2N\}_2]$ (**1**)

Figure S3. XRD pattern of TG residue of $[Me_2Sn\{2\text{-}SeC_5H_2(Me\text{-}4,6)_2N\}_2]$ (**1**) obtained at 800°C .

Figure S4. Deconvolution of pXRD peaks (2θ; 30-31.6°) of tin selenide material synthesized in DDT

Figure S5. EDS spectra of tin selenide nanostructures obtained by thermolysis of $[Me_2Sn\{2\text{-}SeC_5H_2(Me\text{-}4,6)_2N\}_2]$ (**1**) in (a) DDT, (b) OAm+DDT (1:1, v/v) respectively.

Figure S6. EDS spectra of SnSe nanostructures obtained by (a) pyrolysis of **1** and thermolysis of **1** in (b) OAm and (c) ODE respectively.

Figure S7. 2-D Elemental mapping of SnSe nanostructures obtained by (a) pyrolysis of **1** and thermolysis of **1** in (b) OAm and (c) ODE respectively.

Figure S8. SAED pattern of SnSe nanostructures obtained by (a) pyrolysis of **1** and thermolysis of **1** in (b) OAm and (c) ODE respectively.

Figure S9. (a) pXRD pattern, (b) FT-IR spectra, (c) SEM micrograph and (d) EDS spectra of electrode after 100 cycles.

Figure S10. (a) Cycling, coulombic efficiency and normalized capacity of full cell $LiNi_{0.6}Mn_{0.2}Co_{0.2}O_2$ // SnSe at current density 100 mAg^{-1} and (b) Cycling and coulombic efficiency of $LiNi_{0.6}Mn_{0.2}Co_{0.2}O_2$ at current density 100 mAg^{-1}.

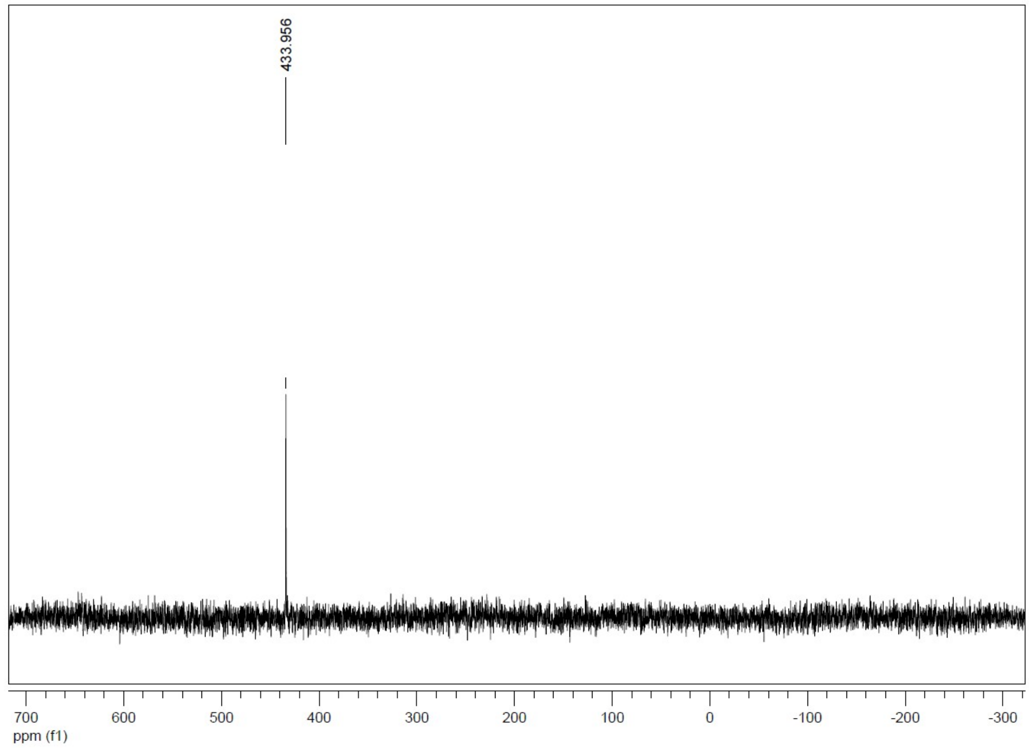

Figure S1 . $^{77}Se\{^{1}H\}$ NMR spectra of bis(4,6-dimethyl-2-pyridyl)diselenide

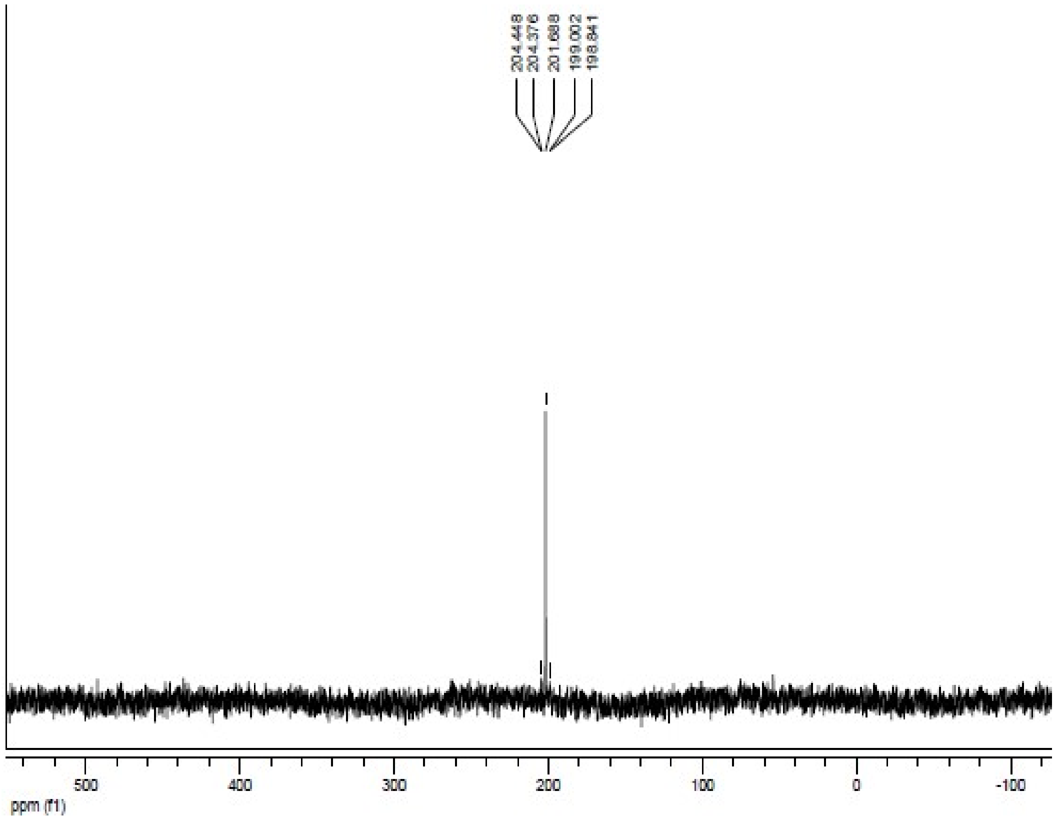

Figure S2. $^{77}Se\{^{1}H\}$ NMR spectra of $[Me_2Sn\{2\text{-}SeC_5H_2(Me\text{-}4,6)_2N\}_2]$ (**1**)

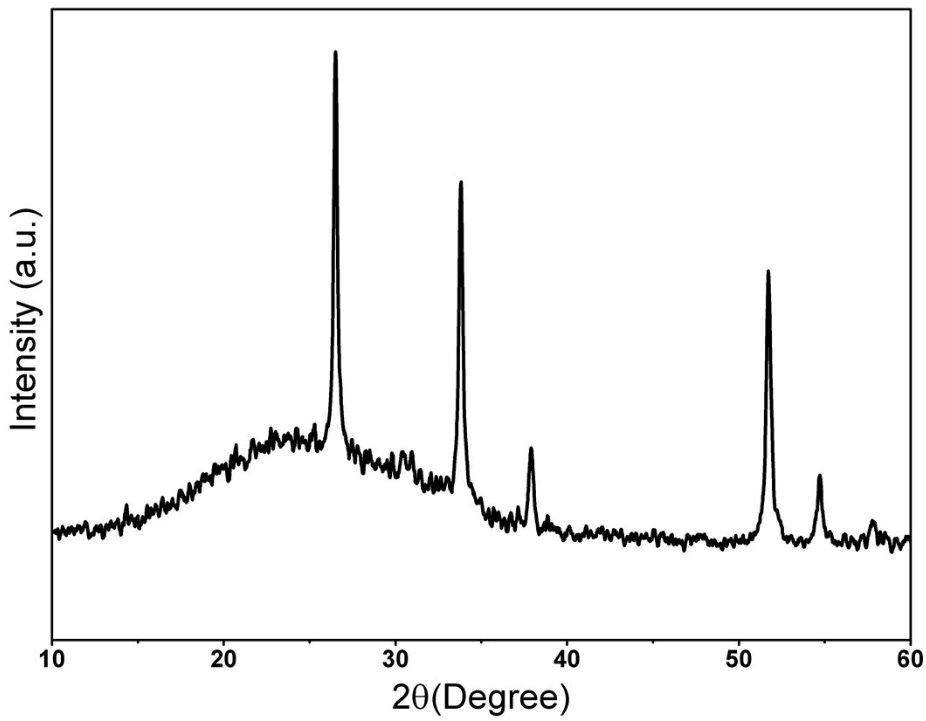

Figure S3. XRD pattern of TG residue of [$Me_2Sn\{2\text{-}SeC_5H_2(Me\text{-}4,6)_2N\}_2$] (**1**) obtained at 800°C.

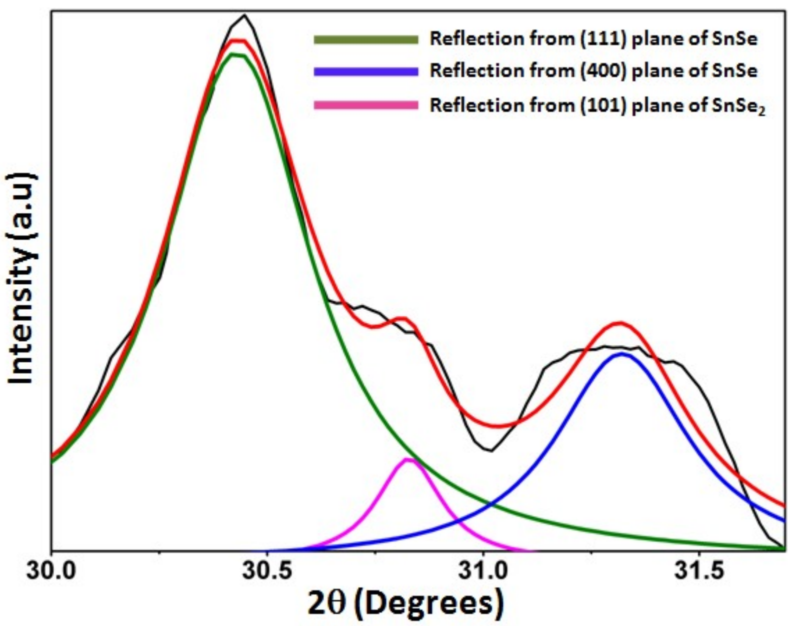

Figure S4. Deconvolution of pXRD peaks (2θ; 30-31.6°) of tin selenide material synthesized in DDT

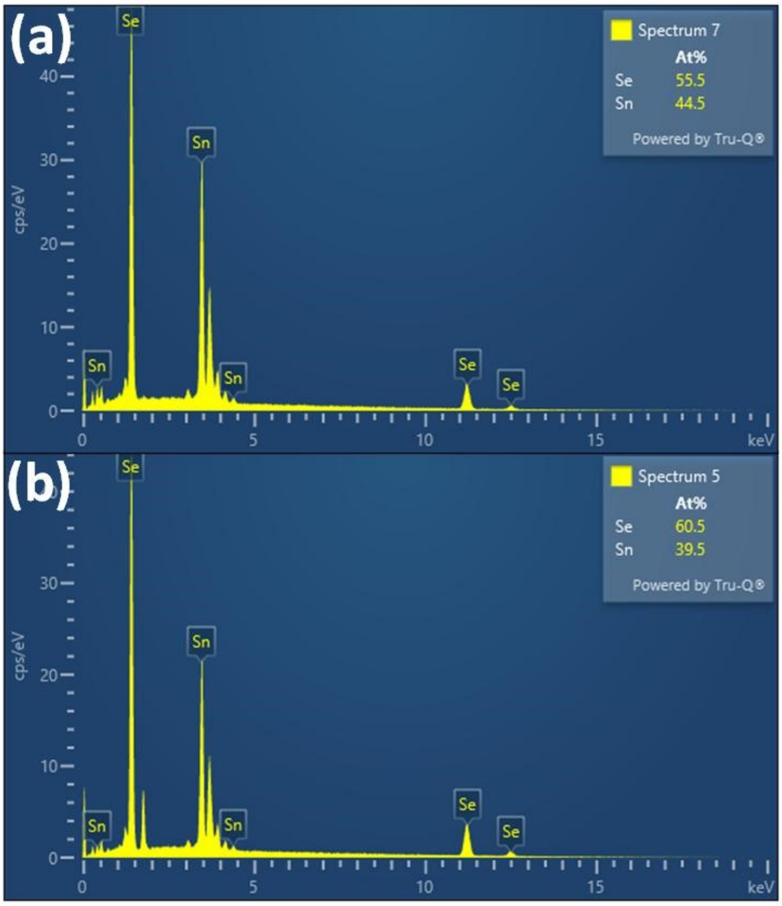

Figure S5. EDS spectra of tin selenide nanostructures obtained by thermolysis of [$Me_2Sn\{2\text{-}SeC_5H_2(Me\text{-}4,6)_2N\}_2$] (**1**) in (a) DDT, (b) OAm+DDT (1:1, v/v) respectively.

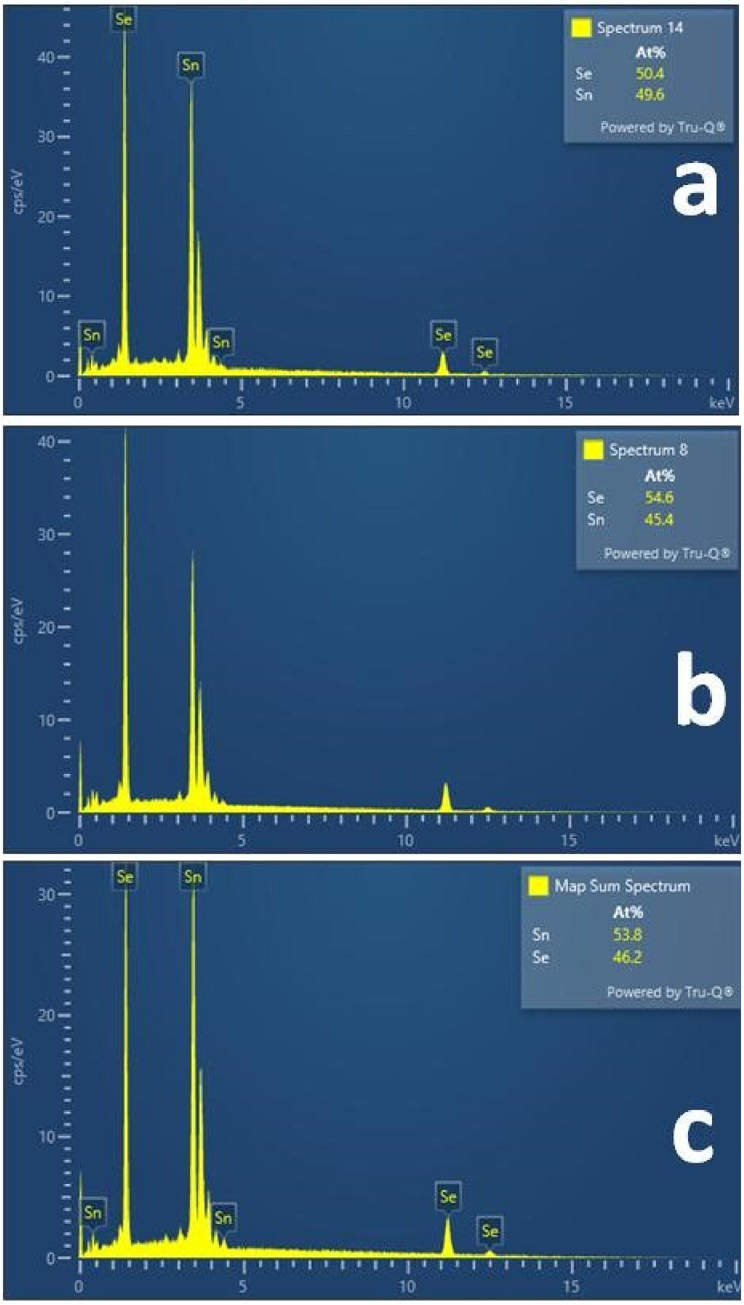

Figure S6. EDS spectra of SnSe nanostructures obtained by (a) pyrolysis of **1** and thermolysis of **1** in (b) OAm and (c) ODE respectively.

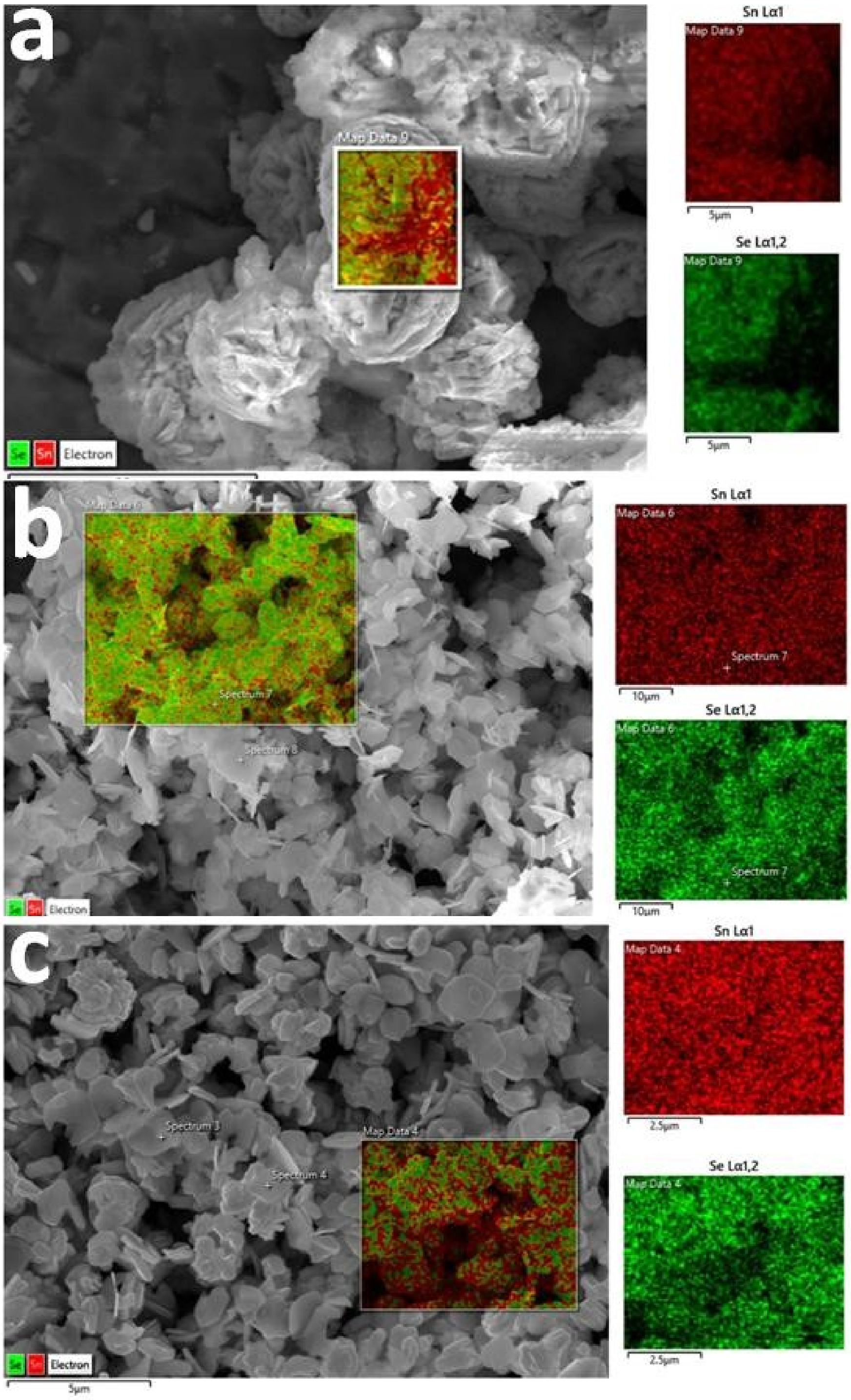

Figure S7. 2-D Elemental mapping of SnSe nanostructures obtained by (a) pyrolysis of **1** and thermolysis of **1** in (b) OAm and (c) ODE respectively.

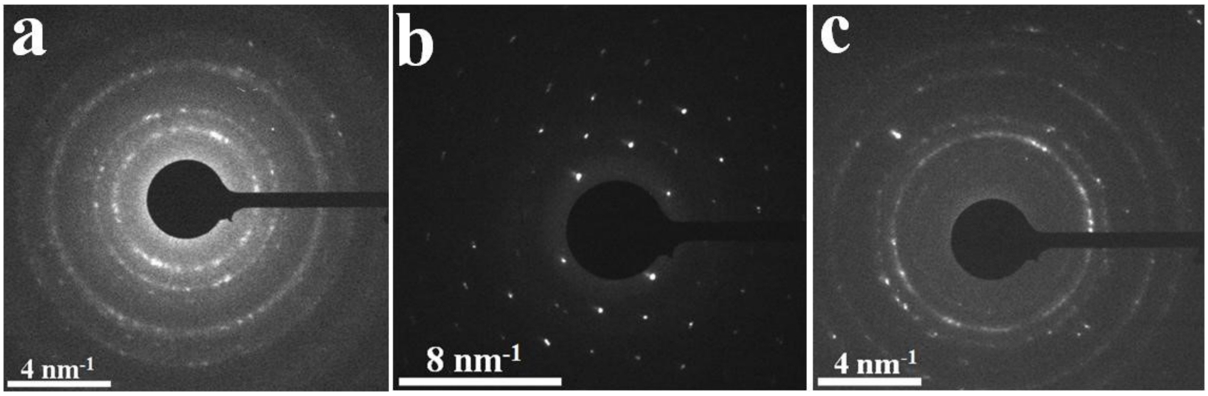

Figure S8. SAED pattern of SnSe nanostructures obtained by (a) pyrolysis of **1** and thermolysis of **1** in (b) OAm and (c) ODE respectively.

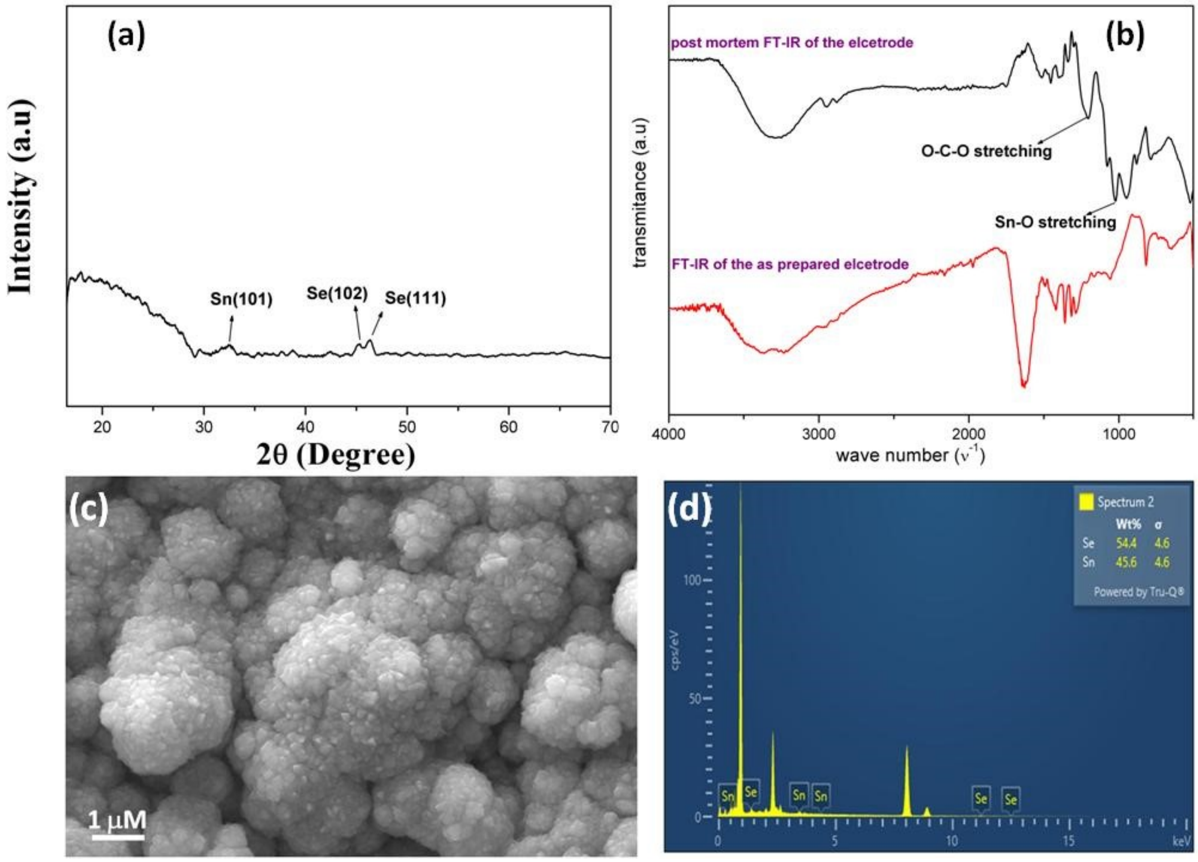

Figure S9. (a) pXRD pattern, (b) FT-IR spectra, (c) SEM micrograph and (d) EDS spectra of electrode after 100 cycles.

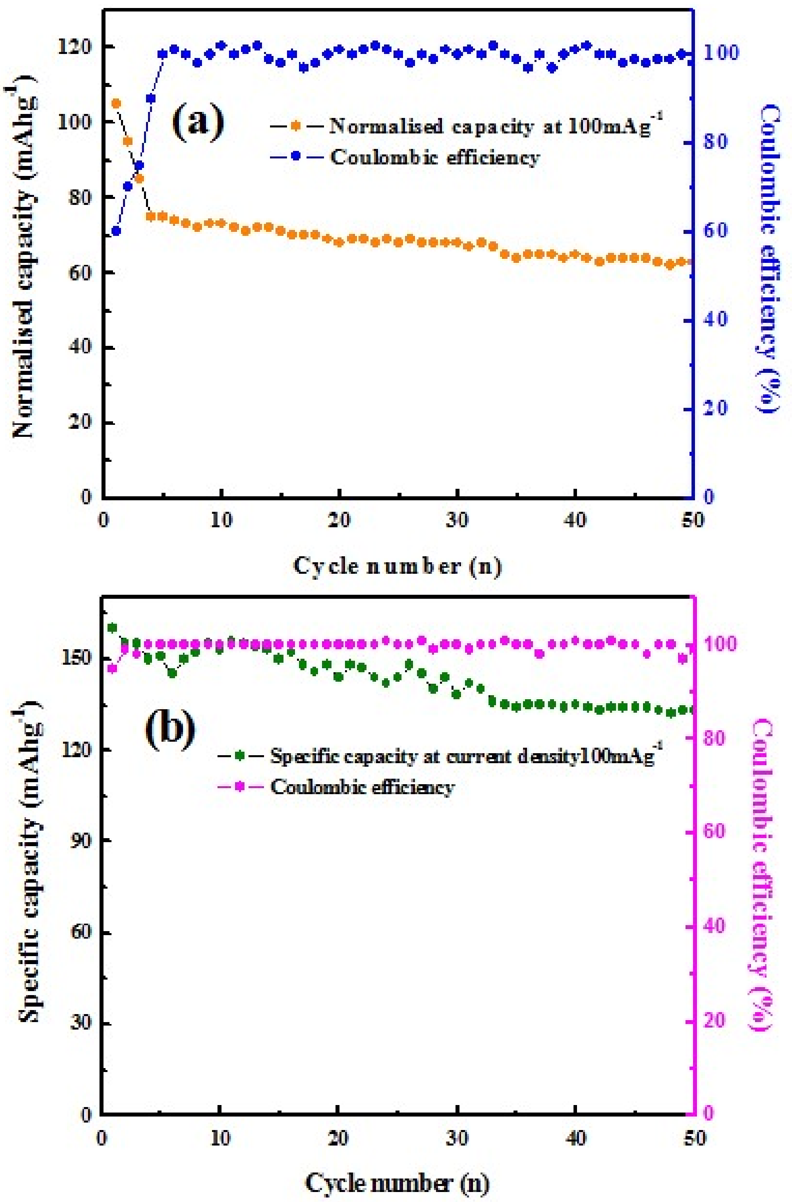

Figure S10. (a) Cycling, coulombic efficiency and normalized capacity of full cell $LiNi_{0.6}Mn_{0.2}Co_{0.2}O_2$ // SnSe at current density 100 mAg^{-1} and (b) Cycling and coulombic efficiency of $LiNi_{0.6}Mn_{0.2}Co_{0.2}O_2$ at current density 100 mAg^{-1}.